Statetostate dynamics of H+HX collisions. II. The H+HX→HX°+H (X=Cl,Br,I) reactive exchange and inelastic collisions at 1.6 eV collision energy

Pamela M. Aker, Geoffrey J. Germann, Kevin D. Tabor, and James J. Valentini

Citation: The Journal of Chemical Physics **90**, 4809 (1989); doi: 10.1063/1.456693
View online: http://dx.doi.org/10.1063/1.456693
View Table of Contents: http://scitation.aip.org/content/aip/journal/jcp/90/9?ver=pdfcov
Published by the AIP Publishing

State-to-state dynamics of H+HX collisions. II. The H+HX→HX†+H (X=Cl,Br,I) reactive exchange and inelastic collisions at 1.6 eV collision energy

Pamela M. Aker, Geoffrey J. Germann, Kevin D. Tabor, and James J. Valentini
Department of Chemistry, University of California, Irvine, California 92717

(Received 28 November 1988; accepted 13 January 1989)

We report measurement of product state distributions for the rotationally and/or vibrationally excited HX formed in collisions of translationally hot H atoms with HX (X = Cl, Br, and I) at 1.6 eV collision energy. The product state distributions are probed after only one collision of the fast H atom, using coherent anti-Stokes Raman scattering spectroscopy. Whether proceeding by inelastic collisions or reactive exchange, the transfer of translational energy to vibrational and rotational energy is quite inefficient in H + HX collisions at 1.6 eV. For all three hydrogen halides only 2–3% of the initial translational energy appears as HX vibration. For H + HCl only 6% of the initial energy is converted to HCl rotational energy, while for H + HBr and H + HI, this percentage is twice as large, 11–12%, but still small. The indistinguishability of the two H atoms involved makes it impossible to distinguish reactive exchange from inelastic energy transfer in these H + HX collisions. However, the difference in rotational energy partitioning for H + HBr and H + HI as compared with H + HCl, suggests that reactive exchange is dominant in the former and inelastic energy transfer dominates in the latter. The total cross sections for the combined energy transfer/reactive exchange do not change much with the identity of X, being 13 ± 3, 11 ± 2, and 11 ± 2 Å^2, for H + HCl, H + HBr, and H + HI, respectively.

I. INTRODUCTION

Collisions of translationally hot H atoms with various small molecules has recently been the focus of many theoretical[1–16] and experimental[17–42] investigations. Hydrogen atom reactions with small molecules are appealing theoretically because the potential energy surfaces for these small systems are relatively easy to calculate, making the systems amenable to a detailed investigation of the dynamics. They are appealing from an experimental perspective as well, for pulsed UV photolysis of hydrides provides an efficient method for generating H atoms over a wide range of translational energy. Copious quantities of H atoms can be produced in a time short compared to collision times in gases at pressures of a few Torr or less, making time-resolved and, more importantly, single-collision studies of the dynamics possible.

The H + HX systems (X = F,Cl,Br,I) present a particularly attractive set of reactions to study, because they afford the opportunity to investigate experimentally, at the state-to-state level, the dynamical consequences of the competition between distinct multiple product channels, and the influence of potential energy surface features and mass effects on this competition. In collisions of a hydrogen atom with a hydrogen halide there are three possible product channels: Inelastic scattering,

$$H' + HX(v, J) \rightarrow H' + HX(v', J'); \quad (1)$$

hydrogen atom exchange,

$$H' + HX(v, J) \rightarrow H'X(v', J') + H; \quad (2)$$

and hydrogen atom abstraction,

$$H' + HX(v, J) \rightarrow H'H(v', J') + X. \quad (3)$$

Variation of the identity of the reactant hydrogen halide provides the means to vary the energetics of the abstraction reaction without significantly altering the kinematics of any of the collision processes, since the reduced masses of both reactants and products for all three channels are essentially independent of the mass of the halogen. Similarly, for the exchange reaction, variation of the identity of the reactant hydrogen halide allows variation in the height of the barrier to reaction, without changing either the kinematics or energetics of the exchange reaction and inelastic collisions.

Such an integrated study is possible only if a "universal" spectroscopic technique—one that possesses the capability for state-resolved detection of all the HX species and the H_2 product as well—can be implemented experimentally under essentially single-collision conditions. Coherent anti-Stokes Raman scattering (CARS) spectroscopy[43] provides just such a capability, and we have used it to investigate the dynamics of reactions (1)–(3) under single-collision conditions. In the preceding paper we described our studies of the hydrogen atom abstraction reactions, Eq. (3). In this report we describe an integrated study of the dynamics of the inelastic and hydrogen-atom-exchanging collisions of H with HCl, HBr, and HI.

The potential energy surfaces for the H + HX systems calculated by Baer and Last[44] provide a basis for formulating some expectations about the dynamics of the reactions. These DIM-3C surfaces are only approximate, but are useful nonetheless. A summary of the energetics and classical barrier heights of the exchange channel for the H + HX reactions is given in Table I, while Table II shows the differences in saddle point geometries for the reactive exchange. The calculated barriers are 1.45, 0.54, 0.48, and 0.42 eV for HFH, HClH, HBrH, and HIH, respectively. Note that the vari-

 0021-9606/89/094809-10$02.10

TABLE I. Energetics of the H′ + HX→H′X + H reactions. All energies are given in eV.

Hydrogen halide	ΔH	$E_b(\theta = 180°)$[a]	$\langle E_b(\theta)\sin\theta\rangle$[b]
HF	0.0	1.45	1.87
HCl	0.0	0.54	1.17
HBr	0.0	0.48	1.00
HI	0.0	0.42	0.82

[a] Collinear barrier heights from Ref. 44.
[b] Weighted average of the barrier height over the range $\theta = 180°$ to $\theta = 90°$, data from Ref. 44.

ation in barrier height and saddle point geometry with variation of the identity of X is not nearly as great for the exchange reactions as it is for the abstraction reactions, since the thermochemistry is the same for all the exchange reactions, while there are large changes in both the magnitude and sign of ΔH_{rxn} for the abstraction channel. The DIM-3C surfaces of Baer and Last have collinear minimum energy paths for H + HI, HBr, and HCl exchange reactions and the bend potential becomes steeper along the series I→Cl. The HFH system is anomalous, however, in that the minimum energy path does not occur for collinear geometry and the bend potential is quite shallow.

The hydrogen atom reactant and the hydrogen atom in the hydrogen halide reactant cannot be labeled or distinguished in our experiments as they can be in writing out the reactions above, and thus the collisions leading to inelastic energy transfer cannot be distinguished from those that lead to hydrogen atom exchange. Reactions of D with HX or H with DX would remove this ambiguity, but at the cost of the geometric and kinematic symmetry in the collisions, and these have not yet been done in our lab. However, as discussions in this paper will show, the v', J' distributions provide information that allows some resolution of the indistinguishability of the inelastic and exchange processes. In particular, the extreme light–heavy–light mass combination of the inelastic and reactive exchange collisions makes the rotational distributions distinguishing. For example, Baer[46] has pointed out that on an isotropic potential energy surface angular momentum conservation for this mass combination dictates that for the inelastic product the distribution over product rotational states is determined by the distribution of reactant rotational angular momentum, while for the reactive exchange product the rotational state distribution depends on the distribution of the reactant orbital angular momentum.

TABLE II. Saddle point geometries for the H′ + HX→H′X + H reactions. All distances are given in Å.

Hydrogen halide	r(H–X)[a]	Δr(H–X)[b]
HF	1.12	0.20
HCl	1.47	0.20
HBr	1.60	0.19
HI	1.78	0.17

[a] Saddle point bond lengths from Ref. 44.
[b] Saddle point bond length minus the equilibrium bond length of the diatom, using the equilibrium bond lengths from Ref. 45.

Previously, infrared (IR) chemiluminescence experiments have been used to investigate the production of vibrationally excited products via $T \rightarrow V$ energy transfer and hydrogen atom exchange reaction in H + HF,[41] H + HCl,[23] and H + HBr.[22] In addition, CARS has been used to study the energy transfer and hydrogen atom abstraction in H + HBr collisions.[24] However, the series of experiments reported in this paper and the one that precedes it are the first studies that probe the complete rotational and vibrational energy distributions from all product channels in H + HX collisions, and the first to be done under single-collision conditions.

The experiments presented here are carried out at 1.6 eV collision energy. We use 266 nm photolysis of HI to generate translationally hot H atoms that give an H + HX collision energy of 1.6 eV. Highly time-resolved CARS spectroscopy is used to record spectra of the rotationally and/or vibrationally excited HX product ($HX^\dagger$) of Eqs. (1) and (2) after a single collision of the hot H atom. Our results show that the HX product, whether it is being formed by inelastic energy transfer or by reactive exchange, is created with only modest amounts of rotational and vibrational excitation, although the cross section for this small energy transfer is significant, $\approx$10–15 Å^2.

II. EXPERIMENT

A combination of UV photolytic generation of fast H atoms and coherent anti-Stokes Raman scattering is used to measure the spectra of rotationally and/or vibrationally excited HX created by inelastic energy transfer and reactive exchange in H + HX collisions at 1.6 eV. The experimental approach, apparatus and data analysis are the same as those described in detail in the preceding paper on the H + HX→H_2 + X reactions. The translationally hot H atoms are generated by 266 nm photolysis of HI, which yields H atoms with two distinct laboratory velocities, 1.75×10^6 and 1.13×10^6 cm s^{-1}, associated with the production of I($^2P_{3/2}$) and I($^2P_{1/2}$), respectively, with quantum yields of 0.66 and 0.34, respectively.[47] These give H + HX collision energies of 1.6 and 0.68 eV. The 3.5 ns delay between the photolysis pulse and the CARS probe pulse allows only a single H + HX collision at these velocities. The $HX^\dagger$ products we observe are those produced by H atom collisions with HX at 1.6 and 0.68 eV relative energies, only. Reaction of less energetic H atoms, produced by collisional cooling, is not significant on our experimental time scale. Even though the experiments are carried out under single-collision conditions, the presence of H atoms giving two different collision energies introduces some ambiguity into the interpretation of the results. As discussed in Sec. IV, however, the small quantum yield for the slower H atoms and their small contribution to product formation, relative to that of the faster H atoms, makes the $HX^\dagger$ we observe almost completely those from the 1.6 eV collisions.

In the preceding paper we documented the detection of H + HX→H_2 + X reaction products under relaxation-free conditions in part by reference to the known very slow self-

relaxation of vibrationally or rotationally excited H_2. Here we are detecting hydrogen halides, for which the rotational and vibrational relaxation are much faster, so some further documentation of relaxation-free conditions is necessary. Rotational relaxation will be the most facile, so it will suffice to show that it is not significant under our experimental conditions. We will consider only $HCl^{\dagger}$ relaxation, HI and HBr relaxation is expected to be slower as the number of collisions these heavier molecules suffer will be smaller due to their slower velocities.

Rohlfing, Chandler, and Parker[48] have recently measured the rates of state-to-state rotational relaxation in HCl–HCl collisions. These measurements were made for HCl in rotational states $J \leqslant 7$, and produce a complete matrix of state-to-state rates involving these rotational states. Since the $HCl^{\dagger}$ products we measure here for H + HCl collisions are formed with most probable J of 5–10, we will use the data of Rohlfing *et al.* for relaxation of $J = 7$ to assess the probability of rotational relaxation of our product state distributions. More specifically, we will use the measured rate for the relaxation of $J = 7$ to $J = 5$, since a change of J of 2 is about the smallest that would represent a meaningful change in our product state distributions. The reported cross section for the relaxation of $J = 7$ to $J = 5$ is 40 Å^2. This cross section is large, but it implies that under our experimental conditions, $P_{HCl} = 2.5$ Torr, the mean time between these $\Delta J = -2$ relaxing collisions is 45 ns, more than 10 times longer than the 3.5 ns probe delay in our experiments. The reported rotational relaxation cross sections depend on the magnitude of both J and ΔJ, but in no case are the cross sections greater than 130 Å^2, a value which would make the mean time between the rotationally relaxing collisions 15 ns under the conditions of our experiments.

The best evidence for our claim that the product state distributions that we measure are unrelaxed comes from actual measurement of $HCl^{\dagger}$ product state distributions as a function of HCl pressure. For HCl sample pressures of 1.5 Torr and 2.5 Torr the measured HCl rotational and vibrational distributions are the same, within the signal to noise of the experiments.

III. RESULTS

A. Spectra and analysis

The measured CARS spectrum of the HCl product of H + HCl collisions is shown in Fig. 1, while Figs. 2 and 3 show analogous spectra of HBr and HI products. The *Q*-branch transitions are labeled with the quantum numbers identifying the origin of each product peak. Unlabeled peaks in the spectrum are due to *O*-branch transitions of reactant HX in thermally populated $v = 0$ rotational states. The CARS spectra of HCl and HBr show line splittings due to the presence of two common halogen atom isotopes of both Cl (^{35}Cl,^{37}Cl) and Br(^{79}Br,^{81}Br).

For H + HCl, rotational states up to $J' = 17$ in $v' = 0$ and $J' = 10$ in the $v' = 1$ level are populated by the reaction. Although collisions of HCl with 1.6 eV H atoms are energetic enough to yield HCl product in $v' = 4$, we could observe no product in vibrational states $v' > 1$. For H + HBr collisions at 1.6 eV, for which population up to $v' = 5$ is energetically possible, we similarly observe population only in the $v' = 0$ and 1 levels. The observed maximum J' state seen for $v' = 0$ is 27 and for $v' = 1$ it is 19. Although states up to $v' = 6$ are energetically accessible in the H + HI collisions, product population is observed only in $v' = 0$, 1, and 2. Population in the $v' = 0$ level up to $J' = 35$ is seen. In the $v' = 1$ and 2 levels the maximum rotational states observed are $J' = 26$ and $J' = 20$, respectively. A few lines in the $v' = 3$, low J' region are evident, but the signal-to-noise ratio for these peaks is small. As a result, populations in the $v' = 3$ level cannot be accurately measured and only an upper limit of the population in this vibrational state can be established. A new set of rotational constants for the HI had to be generated to assign the spectrum. These new constants will be published in a future paper.[49]

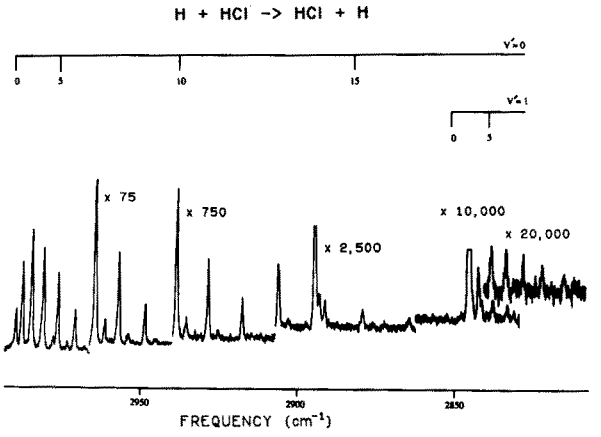

FIG. 1. CARS spectrum of the HCl product of H + HCl collisions at 1.6 eV. The rotational quantum numbers identifying the *Q*-branch transitions for the $v' = 0$ and 1 levels of HCl are given at the top of the diagram. The unlabeled peaks are $v = 0$, $J < 9$ *O*-branch transitions of the HCl reactant.

These spectra are analyzed as described in the preceding

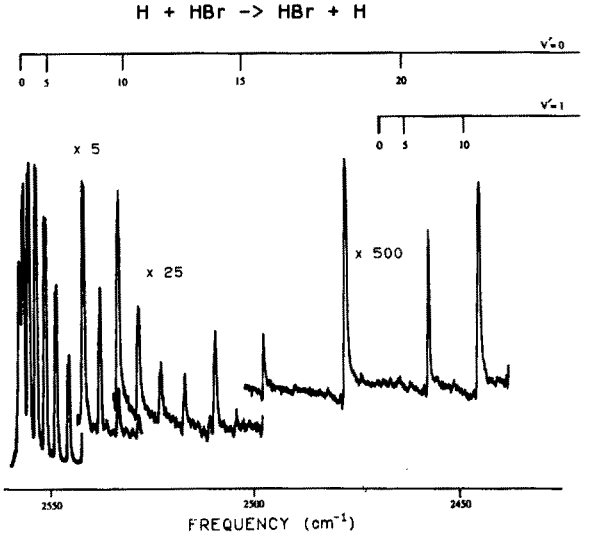

FIG. 2. CARS spectrum of the HBr product of H + HBr collisions at 1.6 eV. The rotational quantum numbers identifying the *Q*-branch transitions for the $v' = 0$ and 1 levels of HBr are given at the top of the diagram. The unlabeled peaks are $v = 0$, $J < 10$ *Q*-branch transitions of the HBr reactant.

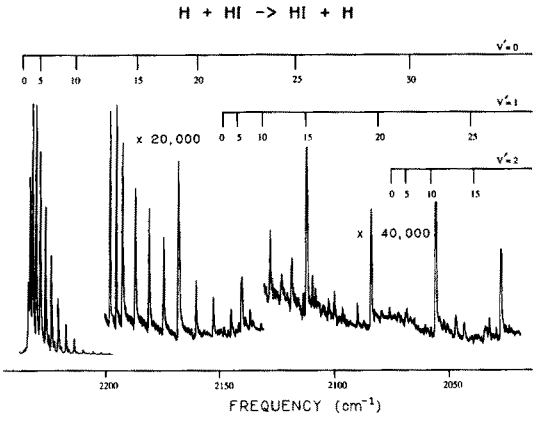

FIG. 3. CARS spectrum of the HI product of H + HI collisions at 1.6 eV. The rotational quantum numbers identifying the Q-branch transitions for the $v' = 0$, 1, and 2 levels of HI are given at the top of the diagram. The unlabeled peaks are $v = 0$, $J < 12$ O-branch transitions of the HI reactant.

paper to yield individual quantum state populations, $N(v', J')$, for the $HX^{\dagger}$ collision products.

B. Absolute reaction cross sections

Absolute cross sections for the $H + HX \rightarrow HX^{\dagger} + H$ collisions are determined by the relations

$$\sigma(v', J') = [HX(v', J')]/[HX]_0[H]_0 v_{rel} \Delta t \qquad (4)$$

and

$$\sigma_{tot} = \sum_{v', J'} \sigma(v', J'), \qquad (5)$$

where [ ] denotes concentration in particles cm^{-3}, v_{rel} is the collision velocity (1.76×10^6 cm s^{-1}) and Δt is the time delay between the photolysis and probe pulses (3.5 ± 0.4 ns). The concentration of H atoms is determined by the difference of CARS spectra of HI recorded with and without photolysis, together with a capacitance manometry measurement of the HI pressure (absolute number density). Capacitance manometry also gives the pressure (absolute number density) of the HX reactant. Similarly, absolute number densities of the HX products are extracted by calibration of the CARS spectrum against CARS signal intensities for HX under conditions where the molecular density is known.

In our experiment the measured spectrum in the $v' = 0$, low J' region of HX contains contributions from both the HX populated by the reaction and unreacted HX. The population due to reaction was determined by extrapolating the product distributions from $J' > 15$, 12, and 8 for HI, HBr, and HCl, respectively, to the low J' region using a linear rotational surprisal analysis.[50] This analysis gives cross sections for the $H + HX \rightarrow HX^{\dagger} + H$ reaction/inelastic energy transfer of 13 ± 3, 11 ± 2, and 11 ± 2 Å^2 for X = Cl, Br, and I, respectively. Within the experimental signal to noise, the cross sections are identical. We justify the extrapolation procedure by noting that the HX rotational state populations in all vibrational states fit a linear surprisal function very well (see the following subsection), and in the $v' = 0$ level there are a large number of rotational states for which the only contribution to the population comes from reactive and inelastic collisions. As a result, an accurate determination of the $v' = 0$ rotational surprisal parameter is possible and extrapolation of the rotational state population distribution back to the thermally populated low J' states in $v' = 0$ is fairly reliable. However, this procedure probably underestimates the contribution from collisions that are vibrationally adiabatic and only slightly rotationally inelastic. Hence, for the $HX^{\dagger}$ product, the $\sigma(v', J')$ are more accurate than σ_{tot}.

C. Product rotational and vibrational state distributions

The measured rotational state distributions in the $v' = 0$ and 1 levels of the HCl and HBr products are given in Figs. 4 and 5, respectively. The rotational distributions measured in the $v' = 0$, 1, and 2 levels of the HI product are shown in Fig. 6. The error bars in these figures and all other figures represent plus-or-minus one standard deviation of uncertainty. Although plotted as relative population distributions, the data actually represent absolute partial cross sections. Conversion to absolute units can be made using the fact that "10" in the arbitrary units of Figs. 4, 5, and 6 is equivalent to 0.19 ± 0.02, 0.63 ± 0.08, and 0.45 ± 0.02 Å^2, respectively.

For each HX product the rotational distribution within each vibrational level was fit to a linear rotational surprisal.[50] The best-fit surprisal distributions are given by the solid lines in Figs. 4–6 along with the corresponding rotational surprisal parameters, θ_R. For the HBr product, $\theta_R = 6.3 \pm 2.3$ and 7.3 ± 2.5 for the $v' = 0$ and 1 levels, respectively. For the HI product, $\theta_R = 7.5 \pm 1.1$, 8.2 ± 1.0, and 7.3 ± 1.8 for the $v' = 0$, 1, and 2 levels, respectively. Within the signal to noise of the experiment, the θ_R values calculated for each vibrational level of the HBr and HI products are the same, indicating that a single θ_R is adequate to describe the rotational energy disposal in the reactions. For the HBr product, the average θ_R is 6.8 ± 0.7, for the HI product the average θ_R is 7.6 ± 0.5. These large positive values of θ_R

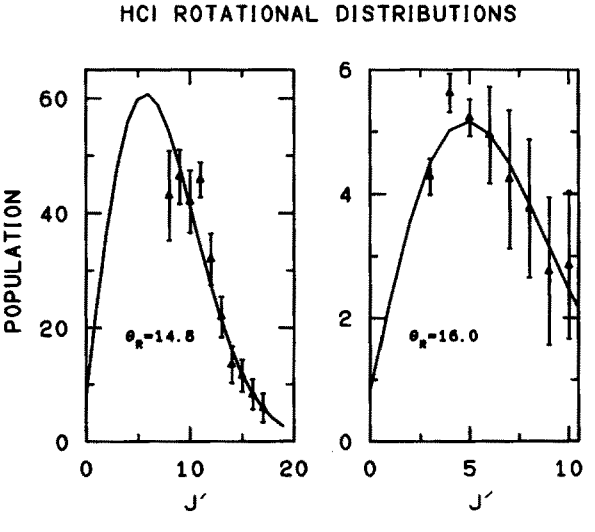

FIG. 4. Rotational state distributions for the HCl product of H + HCl collisions at 1.6 eV. The symbols are the measured populations. The solid lines are the linear rotational surprisal best fits to the measured distributions, with the surprisal parameters given.

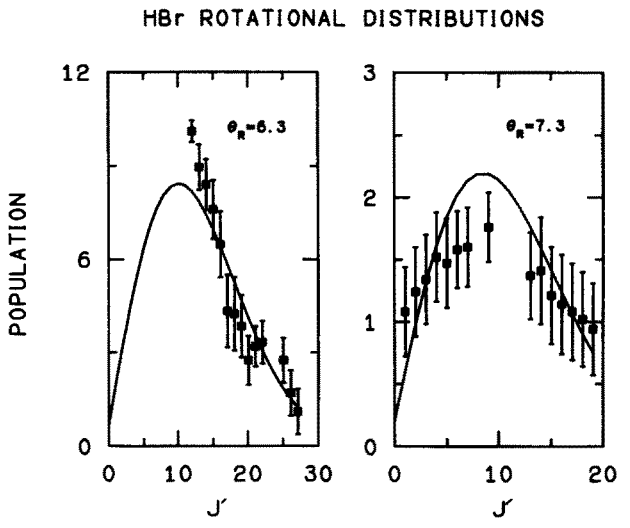

FIG. 5. Rotational state distributions for the HBr product of H + HBr collisions at 1.6 eV. The symbols are the measured populations. The solid lines are the linear rotational surprisal best fits to the measured distributions, with the surprisal parameters given.

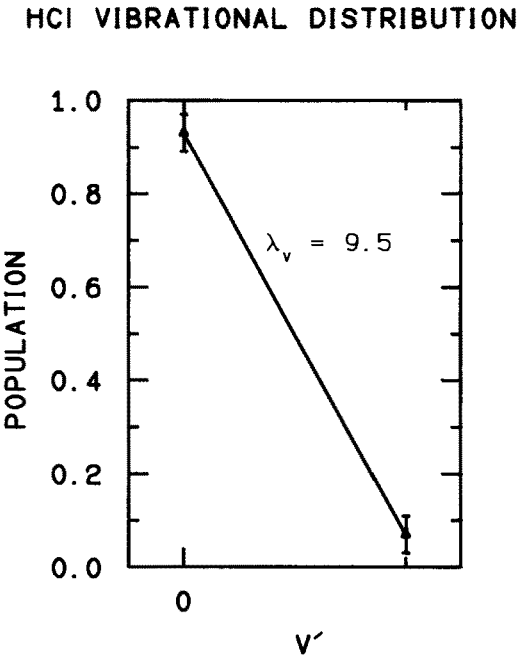

FIG. 7. Vibrational state distribution of the HCl product of H + HCl collisions at 1.6 eV. The symbols with error bars are the measured populations, while the solid line is the linear vibrational surprisal fit to the data, with the surprisal parameter given.

imply that there is a dynamical bias against population of high rotational states of the HX product. This is further emphasized by the low value of f'_r, the fraction of the available energy in product rotation, which is only 0.12 ± 0.02 and 0.11 ± 0.02 for the HBr and HI products, respectively.

As with the HI and HBr products, the θ_R values observed in the $v' = 0$ and 1 levels of the HCl product, 14.8 ± 2.6 and 16.0 ± 6.5, respectively, are similar, again suggesting that a single θ_R can be used to describe the rotational energy partitioning in the H + HCl→HCl + H reaction, but the average θ_R, 15.4 ± 0.8, is over *2 times larger* than the average θ_R's observed for the HBr and HI reactions. In fact, the HCl rotational surprisal parameters are the largest we have ever measured for any H atom reaction at any collision energy and suggest that the bias against rotational excitation in $H + HCl \rightarrow HCl^{\dagger} + H$ collisions is much stronger than in $H + HBr \rightarrow HBr^{\dagger} + H$ and $H + HI \rightarrow HI^{\dagger} + H$ collisions. The f'_r value measured for the HCl reaction is 0.06 ± 0.02, a value one-half that observed for the HBr and HI reactions.

The HCl, HBr, and HI product vibrational distributions are shown in Figs. 7, 8, and 9, respectively. The vibrational distributions are obtained by summing the population of the

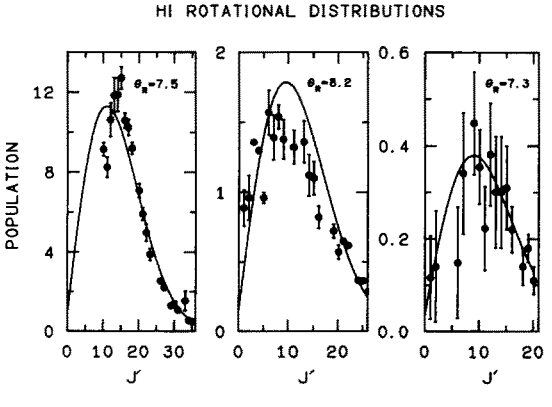

FIG. 6. Rotational state distributions for the HI product of H + HI collisions at 1.6 eV. The symbols are the measured populations. The solid lines are the linear rotational surprisal best fits to the measured distributions, with the surprisal parameters given.

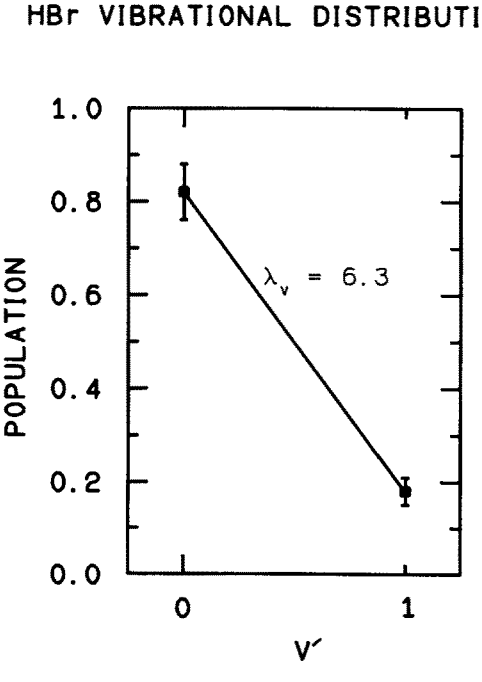

FIG. 8. Vibrational state distribution of the HBr product of H + HBr collisions at 1.6 eV. The symbols with error bars are the measured populations, while the solid line is the linear vibrational surprisal fit to the data, with the surprisal parameter given.

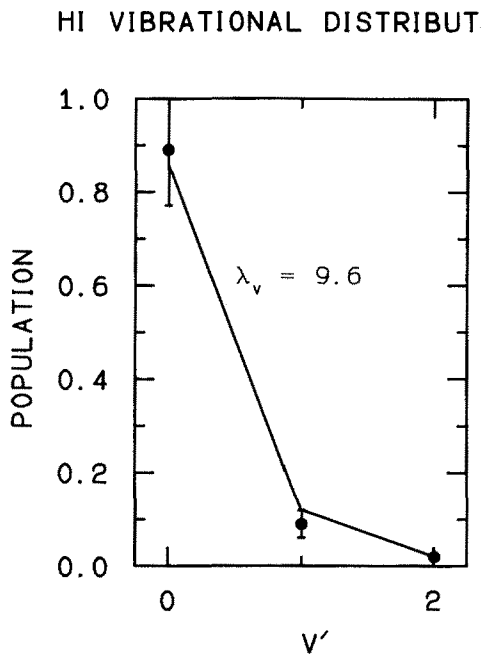

FIG. 9. Vibrational state distribution of the HI product of H + HI collisions at 1.6 eV. The symbols with error bars are the measured populations, while the solid line is the linear vibrational surprisal fit to the data, with the surprisal parameter given.

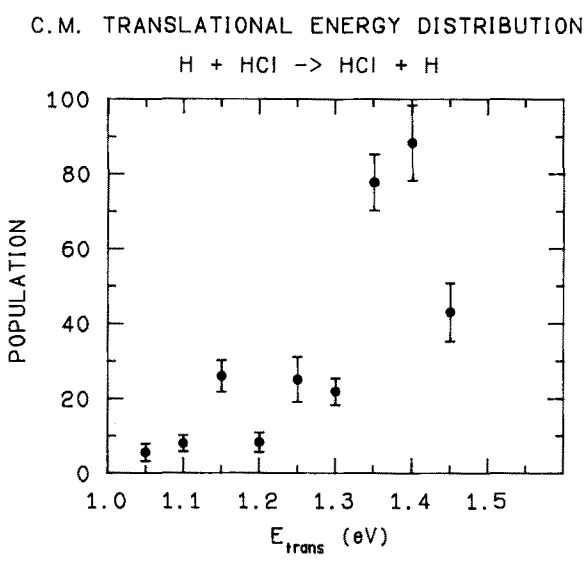

FIG. 10. Product center-of-mass translational energy distribution for H + HCl→HCl + H. The distribution is obtained by inverting the measured HCl product quantum state distributions.

individual rotational states within each vibrational level. For the sums, we use the best-fit linear rotational surprisal population distributions, rather than the experimentally measured ones. This has no effect other than to fill in the populations for rotational states not actually observed in the experiment, principally the low J' of $v' = 0$, for which the large thermal reactant background population precludes direct determination of the product populations. Also included in Figs. 7–9 are the best-fit linear vibrational surprisal distributions,[50] which are given by the solid lines.

For the HCl product, the populations of the $v' = 0$ and 1 levels are 0.93 ± 0.03 and 0.07 ± 0.01, respectively, for which the linear vibrational surprisal parameter, λ_v is 9.5 ± 3.3. The fraction of the available energy that appears as HCl vibration, f_v', is a miniscule 0.02 ± 0.01. The relative populations in the $v' = 0$ and 1 levels of the HBr product are 0.82 ± 0.06 and 0.18 ± 0.03, giving an f_v' value of 0.03 ± 0.01 and a λ_v of 6.3 ± 3.7. For the HI product, the relative populations in the $v' = 0$, 1, and 2 levels are 0.89 ± 0.04, 0.09 ± 0.03, and 0.02 ± 0.01, respectively, corresponding to an f_v' of 0.02 ± 0.01 and a λ_v of 9.6 ± 4.2.

Given the tiny energy disposal in HX vibration and rotation, the H + HX product center-of-mass translational energy distributions must be very near the 1.6 eV of the reactants. The HCl, HBr, and HI center-of-mass translational energy distributions, obtained by inverting the measured HX quantum state distributions and given in Figs. 10, 11, and 12, respectively, show this. For the HCl reaction, the peak of the product translational energy distribution occurs at 1.4 eV, which corresponds to 88% of the initial reactant translational energy, and f_t', the fraction of the total available energy partitioned to translation, is 0.92 ± 0.03. For the HBr reaction the product translational energy distribution peaks at 1.35 eV, corresponding to 84% of the initial translational energy and f_t' is 0.85 ± 0.03. In the H + HI products, the translational energy distribution peaks at 1.4 eV, corresponding to 88% of the initial collision energy, and f_t' is 0.87 ± 0.03.

For comparison purposes, the important parameters of the HX product vibrational and rotational state distributions for all three reactions are given in Table III. It is interesting to note the similarities in the product energy distributions of the HI and HBr products. Within the experimental uncertainty, the energy partitioning in these two reactions is identical. However, the HCl product energy disposal is different, most notably in the rotational energy disposal. We

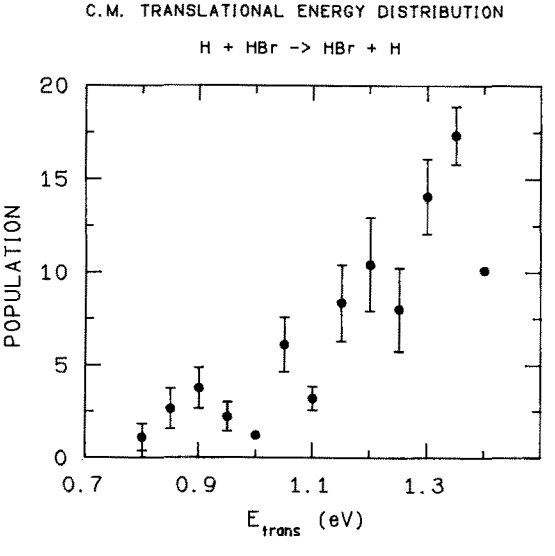

FIG. 11. Product center-of-mass translational energy distribution for H + HBr→HBr + H. The distribution is obtained by inverting the measured HBr product quantum state distributions.

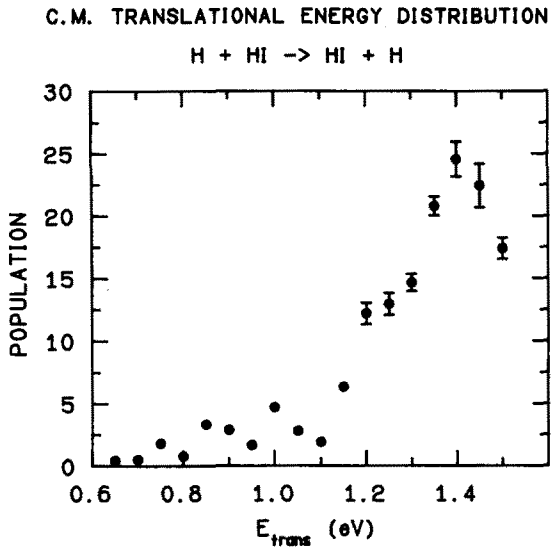

FIG. 12. Product center-of-mass translational energy distribution for H + HI→HI + H. The distribution is obtained by inverting the measured HI product quantum state distributions.

believe that this is due to a difference in the mechanism for energy transfer in the HBr and HI systems and that in the HCl system. This issue will be addressed in the next section.

The surprisal parameters, the f'_t, f'_r, and f'_v values, and the product translational energy distributions all require specification of the total energy for their determination. Since there are two H + HX collision energies in our experiments, 1.6 eV and 0.68 eV, associated with the two HI photolysis channels, H + I($^2P_{3/2}$) and H + I($^2P_{1/2}$), respectively, there is in principle some ambiguity in the values of these parameters that describe the product energy disposal. In practice, however, this ambiguity is not very important. First, the quantum yield[47] for the H + I($^2P_{3/2}$) channel is almost twice that of the H + I($^2P_{1/2}$) channel. Second, by virtue of their greater velocity the 1.6 eV H atoms are much more likely to undergo a collision than the 0.68 eV H atoms. Together, these two factors imply that if the collision cross sections are energy independent the 1.6 eV collisions contribute 75% of the product and the 0.68 eV collisions only 25%. However, the contribution of the 0.68 eV collisions is probably less than this, since the inelastic and reactive exchange cross sections probably increase with increasing collision energy in this energy regime—note (Table I) that the barriers for the exchange reactions are calculated to be between 0.42 and 0.54 eV for collinear geometries, and increase for smaller HXH angles.[44] Consequently, the lower energy collisions probably contribute less than 10% of the HX products we observe, and are of small significance.

IV. DISCUSSION

Our experimental results show that $T \rightarrow V,R$ energy transfer in the H + HX systems, whether it occurs via an inelastic energy transfer or a reactive exchange mechanism, is very inefficient at this collision energy. Only 8% ± 3%, 15% ± 3%, and 13% ± 3% of the initial collision energy is converted to internal excitation of the HCl, HBr, and HI products, respectively, with most of this excitation (6%, 12%, and 11%, respectively) residing in HX rotation. Because isotopic labeling was not used in this experiment, it is not possible to determine unambiguously which mechanism, inelastic or reactive, dominates the dynamics in these systems.

Some insight about the mechanism that dominates the H + HX→HX† + H collisions can be obtained by examining the rotational distributions that arise in the HX products. The distributions show that the ΔJ of the HI and HBr products is significant (Table III), while that of the HCl product is small. For example, in the $v' = 0$ state of the HI and HBr products, population in rotational states as high as $J' = 35$ and 27, respectively, is observed. Rotational states up to $J' = 26$ and $J' = 19$ in the $v' = 1$ HI and HBr levels, respectively, are also seen and in the HI product, rotational states up to $J' = 20$ in the $v' = 2$ level are observed. The average J' measured in the HI and HBr $v' = 0$ product rotational distribution is 11 to 12. The average J of the initial Boltzmann HI and HBr reactant distribution is 4 to 5. Thus, collisions of translationally excited H atoms with HI and HBr excite, on average, 7 quanta of rotational angular momentum, and there is appreciable probability of changing J by more than 20. In contrast, in the HCl product, rotational states only up to $J' = 17$ and 10 in the $v' = 0$ and 1 levels, respectively, is seen and the average J' of the product is only 5. The average J of the initial HCl distribution is 3 to 4. Thus collisions of translationally excited H atoms with HCl excite only 1 to 2 quanta of rotational angular momentum.

It would seem unlikely that the large ΔJ observed in the HI and HBr systems, especially in the HI system, arises from a purely inelastic process. The electron distribution about the HI molecule is expected to be nearly isotropic, since the centers of mass and charge are almost exactly coincident. The difference between the Pauling electronegativities of H(2.1) and I(2.5) is very small, giving the molecule a very small dipole moment, 0.38 debye. Thus, we expect the

TABLE III. Parameters of the product quantum state distributions in H + HX→HX† + H collisions at 1.6 eV collision energy.

Hydrogen halide	f'_r	f'_v	f'_t	$\Delta\langle v\rangle^a$	$\Delta\langle J\rangle_{v'=0}{}^b$	σ_{tot} (Å^2)
HCl	0.06 ± 0.02	0.02 ± 0.01	0.92 ± 0.03	0.07	2	13 ± 3
HBr	0.12 ± 0.02	0.03 ± 0.01	0.85 ± 0.03	0.18	7	11 ± 2
HI	0.11 ± 0.02	0.02 ± 0.01	0.87 ± 0.03	0.13	7	11 ± 2

[a] The change in average vibrational quantum number, $\Delta\langle v\rangle = \langle v'\rangle - \langle v\rangle_0 = \langle v'\rangle - 0 = \langle v'\rangle$.
[b] The change in average rotational quantum number for products in $v' = 0$, $\Delta\langle J\rangle = \langle J'\rangle - \langle J\rangle$.

H + HI intermolecular potential to be nearly isotropic, except at very small separation. This should make it difficult for the H atom to excite rotation in an inelastic collision process, difficult at least to produce the high J' we observe. This leads us to believe that most or all of the experimentally measured HI product results from the reactive exchange process. The HBrH potential is also probably quite isotropic and so it would seem unlikely that the high rotational states of HBr that we observe could be due to inelastic collisions. However, based solely on this, our case for the dominance of reactive exchange is very weak. The increased polarity of the HBr bond compared to that for HI, makes it more difficult to ignore the anisotropy of the H + HBr long-range interaction.

The evidence which best supports the conclusion that reactive exchange dominates $T \rightarrow V,R$ energy transfer in both the H + HI and H HBr systems comes from a comparison of the rotational surprisal parameters measured for the HX product of H + HI, H + HBr, and H + HCl collisions. The average θ_R values measured for the HI and HBr reactions, 7.6 ± 0.5 and 6.8 ± 0.5, respectively, are equal. In contrast, the θ_R value measured for the HCl reaction is more than 2 times as large, 15.4 ± 0.5. This doubling of the rotational surprisal parameter is quite significant. Our studies of the state-to-state dynamics of the H + D_2, H + H_2, and D + H_2 systems, show that the rotational surprisal parameter for inelastic $T \rightarrow V,R$ is almost always about double that for the reactive exchange for a given pair of reactants.[17–20,51,52] We cite these H + H_2 (and isotopic variants) results because the reduced masses of H + H_2 and H + HX are very similar as are the H_2 and HX reduced masses, and the H + H_2 potential energy surface is similar to those for H + HX exchange reactions. The H + H_2 barrier height is 0.43 eV,[53,54] while for H + HX → HX + H the barrier heights (Table I) are 0.54, 0.48, and 0.42 eV for X = Cl, Br, and I, respectively, and all four reactions have collinear minimum energy paths. The factor of 2 difference in θ_R between the H + HCl and the H + HBr and H + HI reactions viewed in comparison to the H + H_2 dynamics thus suggests that inelastic $T \rightarrow V,R$ dominates the dynamics in the H + HCl system while the reactive exchange mechanism dominates in H + HI and H + HBr collisions.

The recent classical trajectory calculations of reactive exchange and inelastic energy transfer in H + HF collisions by Schatz[16] further support the view that in H + HI → $HI^{\dagger}$ + H and H + HBr → $HBr^{\dagger}$ + H reactive collisions are dominant, while in H + HCl → $HCl^{\dagger}$ + H it is inelastic collisions that are dominant. Schatz found that in inelastic H + HF ($v = 0$, $J = 0$) collisions, $\langle J' \rangle \approx 5$, while in reactive H + HF collisions $\langle J' \rangle \approx 13$, 2.5 times greater. Note that we find $\langle J' \rangle \approx 11$ to 12 for H + HI and H + HBr, while $\langle J' \rangle = 5$ for H + HCl.

The calculations of Baer and Last[44] show that the potential energy surfaces (Table I) for the exchange reactions have significant barriers, with the minimum energy path occurring for collinear HXH geometries. The rotational distributions measured in all vibrational levels of the HI and HBr products support the premise that the minimum energy path occurs for a collinear reaction geometry, since the average rotational surprisal parameter determined for the distributions is very large, $\theta_R = 6.8 \pm 0.5$ and 7.6 ± 0.7, respectively. However, *kinematic* effects may play as important a role as the potential-energy surface in restricting the product rotation in the reaction. For example, the H–IH and H–BrH repulsive energy release in the exit channel should be ineffective in exciting product rotation because the resultant force is directed at the I or Br end of the HI and HBr. This force cannot lead to much rotational excitation then, for it is directed at the center of mass of the HX rotor. This kinematic effect can also explain the small amount of vibrational excitation seen in the HI and HBr products.

While reactive exchange probably dominates the production of rotationally and vibrationally excited HI and HBr in H + HI and H + HBr collisions at 1.6 eV, there certainly may be a contribution from rotationally inelastic collisions to the low J' population in $v' = 0$. The deviation of the observed population distribution from the best-fit linear surprisal curve at J' less than 15 and 12, respectively, may be an indication of this inelastic contribution. For even lower J', those we cannot probe due to the thermal distribution of the reactant, rotationally inelastic collisions are almost certainly the dominant source since inelastic collisions with very small ΔJ should have state-to-state cross sections much larger than those for the exchange reaction at these energies, even if the potential energy surfaces are nearly isotropic.

The 11 ± 2 Å^2 total cross section we report for both the H + HI and H + HBr exchange reactions does not include contributions from these rotationally inelastic, vibrationally adiabatic nonreactive collisions, since it is computed using the linear surprisal description of the large ΔJ measurements to extrapolate the HI and HBr product populations in low J'. With regard to the reactive exchange mechanism, the magnitude of these cross sections may seem large. But, in reality these cross sections are significantly smaller than the estimated hard-sphere elastic H + HI and H + HBr cross sections of 17 and 15 Å^2, respectively [$d_{\text{H-HI}} \sim (d_{\text{H}_2}/2 + d_{\text{Xe}})/2 = 0.23$ nm, $d_{\text{H-HBr}} \sim (d_{\text{H}_2}/2 + d_{\text{Kr}})/2 = 0.22$ nm, $d_{\text{Kr-Kr}} = 0.31$ nm[55]]. In fact, the measured cross sections are about equal to those expected if reaction occurs on every collision in which the H–IH and H–BrH distances reach the H–I and H–Br equilibrium bond lengths of 1.61 and 1.41 Å, respectively. The exchange reaction cross section can be large because the I and Br atoms are such large targets.

If our conclusion that inelastic collisions dominate $T \rightarrow V,R$ in the H + HCl system and reactive exchange dominates $T \rightarrow V,R$ in the H + HI and H + HBr systems is correct, then one must also conclude that this change in dynamics along the series I → Cl does not occur at the expense of the H atom abstraction reaction or alter the abstraction reaction dynamics. The cross sections measured for the abstraction reactions (see preceding paper) in the HI, HBr, and HCl systems are the same, within experimental uncertainty, 2 ± 1 Å^2, 3 ± 1 Å^2, and 2 ± 1 Å^2, respectively. Previous discussions on energy transfer in the H + HCl system (and its isotopic analogs) have suggested that the mechanism for inelastic $T \rightarrow V,R$ involves impulsive momentum transfer between the two H atoms in the system.[26] If the inelastic

$T \rightarrow V,R$ occurs via momentum transfer, then the cross section for the abstraction reaction should decrease as the cross section for inelastic energy transfer increases because the two mechanisms compete for the same geometry of approach. That the cross section for abstraction does not change along the series I→Cl suggests that impulsive momentum transfer is not the mechanism which gives rise to inelastic $T \rightarrow V,R$. Recent studies of inelastic $T \rightarrow V,R$ in the H + HF system, done by Schatz,[16] show that a failed reactive exchange mechanism best describes the dynamics of inelastic $T \rightarrow V,R$. Our observations on the competition between reactive exchange, inelastic $T \rightarrow V,R$ and H atom abstraction in the H + HX series are consistent with this mechanism.

The effect of collisions of the 0.68 eV H atoms on the measured HX quantum state distributions is not known. If the cross sections for both the inelastic and the reactive exchange processes are assumed to be independent of the collision energy then 25% of the measured distribution results from collisions of the slower H atoms. If the HX product is the result of a reactive exchange mechanism, the angular momentum selection rules developed by Baer[46] indicate that the effect of collisions of the slower H atoms would be to shift the rotational distributions to slightly lower J' values. For the inelastic process, these selection rules show that the lower energy collisions would have no effect on the final rotational distributions.

V. CONCLUSION

The first measurements of the complete HCl, HBr, and HI product vibrational and rotational state distributions arising from collision of 1.6 eV H atoms with HCl, HBr, and HI are reported. The experimental results show that $T \rightarrow V,R$ energy transfer in these systems is very inefficient at this collision energy. Only 6%, 12%, and 11% of the initial translational energy is converted to HCl, HBr, and HI rotation, and a mere 2%, 3%, and 2% to vibration, respectively. The HX product quantum state distributions cannot be uniquely assigned to either the reactive exchange or inelastic $T \rightarrow V,R$ mechanisms. However, a comparison of the rotational energy partitioning measured for $H + HI \rightarrow HI^{\dagger} + H$ and $H + HBr \rightarrow HBr^{\dagger} + H$ collisions with that measured for $H + HCl \rightarrow HCl^{\dagger} + H$ collisions suggests that the reactive exchange mechanism dominates the dynamics in the HI and HBr systems, while inelastic $T \rightarrow V,R$ dominates the dynamics in the HCl system.

ACKNOWLEDGMENTS

This work is supported by the Division of Chemical Sciences, Office of Basic Energy Sciences, Office of Energy Research, U.S. Department of Energy.

[1]L. C. Geiger and G. C. Schatz, J. Phys. Chem. **88**, 214 (1984).
[2]L. C. Geiger, C. G. Schatz, and L. B. Harding, Chem. Phys. Lett. **114**, 520 (1985).
[3]N. C. Blais and D. G. Truhlar, Chem. Phys. Lett. **102**, 120 (1983).
[4]J. N. L. Connor and W. J. E. Southall, Chem. Phys. Lett. **123**, 139 (1986).
[5]S. H. Suck Salk, C. R. Klein, and C. K. Lutrus, Chem. Phys. Lett. **110**, 112 (1984).
[6]G. C. Schatz, Chem. Phys. Lett. **108**, 532 (1984).
[7]R. D. Levine and R. B. Bernstein, Chem. Phys. Lett. **105**, 467 (1984).
[8]N. C. Blais, D. G. Truhlar, and B. C. Garrett, J. Chem. Phys. **82**, 2300 (1985).
[9]N. C. Blais and D. G. Truhlar, J. Chem. Phys. **83**, 2201 (1985).
[10]N. C. Blais, R. B. Bernstein, and R. D. Levine, J. Phys. Chem. **89**, 10 (1985).
[11]H. S. Bowers, B. H. Choi, R. T. Poe, and K. T. Tang, Chem. Phys. Lett. **116**, 239 (1985).
[12]G. C. Schatz, M. C. Colton, and J. L. Grant, J. Phys. Chem. **88**, 2971 (1984).
[13]M. C. Colton and G. C. Schatz, J. Chem. Phys. **83**, 3414 (1985).
[14]D. C. Clary, Chem. Phys. Lett. **80**, 271 (1981).
[15]D. C. Clary, Mol. Phys. **44**, 1083 (1981).
[16]G. C. Schatz, J. Chem. Phys. **86**, 6738 (1987).
[17]D. P. Gerrity and J. J. Valentini, J. Chem. Phys. **79**, 5202 (1983).
[18]D. P. Gerrity and J. J. Valentini, J. Chem. Phys. **81**, 1298 (1984).
[19]D. P. Gerrity and J. J. Valentini, J. Chem. Phys. **82**, 1323 (1985).
[20]D. P. Gerrity and J. J. Valentini, J. Chem. Phys. **83**, 2207 (1985).
[21]E. E. Marinero, C. T. Rettner, and R. N. Zare, J. Chem. Phys. **80**, 4146 (1984).
[22]F. Magnotta, D. J. Nesbitt, and S. R. Leone, Chem. Phys. Lett. **83**, 21 (1981).
[23]C. A. Wight, F. Magnotta, and S. R. Leone, J. Chem. Phys. **81**, 3951 (1984).
[24]C. R. Quick and D. S. Moore, J. Chem. Phys. **79**, 759 (1983).
[25]C. A. Wight and S. R. Leone, J. Chem. Phys. **78**, 4875 (1983).
[26]C. A. Wight and S. R. Leone, J. Chem. Phys. **79**, 4823 (1983).
[27]C. A. Wight, D. J. Donaldson, and S. R. Leone, J. Chem. Phys. **83**, 660 (1985).
[28]C. F. Wood, G. W. Flynn, and R. E. Weston, Jr., J. Chem. Phys. **77**, 4776 (1982).
[29]C. R. Quick, R. E. Weston, Jr., and G. W. Flynn, Chem. Phys. Lett. **83**, 15 (1981).
[30]J. O. Chu, C. F. Wood, G. W. Flynn, and R. E. Weston, Jr., J. Chem. Phys. **80**, 1703 (1983).
[31]J. O. Chu, G. W. Flynn, and R. E. Weston, Jr., J. Chem. Phys. **78**, 2990 (1983).
[32]J. O. Chu, C. F. Wood, G. W. Flynn, and R. E. Weston, Jr., J. Chem. Phys. **81**, 5533 (1984).
[33]J. A. O'Neill, J. Y. Cai, C. X. Wang, G. W. Flynn, and R. E. Weston, Jr., J. Chem. Phys. **84**, 50 (1986).
[34]S. Datta, R. E. Weston, Jr., and G. W. Flynn, J. Chem. Phys. **80**, 4071 (1984).
[35]T. H. McGee, R. E. Weston, Jr., and G. W. Flynn, J. Chem. Phys. **83**, 145 (1985).
[36]C. R. Quick and J. J. Tiee, Chem. Phys. Lett. **100**, 223 (1983).
[37]K. Kleinermanns and J. Wolfrum, Chem. Phys. Lett. **104**, 157 (1984).
[38]K. Kleinermanns, E. Linnebach, and J. Wolfrum, J. Phys. Chem. **89**, 2525 (1985).
[39]K. Kleinermanns and J. Wolfrum, Ber. Bunsenges. Phys. Chem. **89**, 316 (1985).
[40]K. Kleinermanns and E. Linnebach, J. Chem. Phys. **82**, 5012 (1985).
[41]L. M. Cousins and S. R. Leone, J. Chem. Phys. **86**, 6731 (1987).
[42]G. Radhakrishnan, S. Buelow, and C. Wittig, J. Chem. Phys. **84**, 727 (1986).
[43]For a review of CARS see J. J. Valentini, in *Spectrometric Techniques*, edited by G. A. Vanasse (Academic, New York, 1985), Vol. 4, Chap. 1.
[44]M. Baer and I. Last, in *Potential Energy Surfaces and Dynamics Calculations*, edited by D. G. Truhlar (Plenum, New York, 1981).
[45]K. P. Huber and G. Herzberg, *Constants of Diatomic Molecules* (Van Nostrand Reinhold, New York, 1979).
[46]M. Baer, Mol. Phys. **26**, 369 (1973).
[47]R. D. Clear, S. J. Riley, and K. R. Wilson, J. Chem. Phys. **63**, 1340 (1975).
[48]E. A. Rohlfing, D. W. Chandler, and D. H. Parker, J. Chem. Phys. **87**, 5229 (1987).
[49]P. M. Aker and J. J. Valentini (unpublished).
[50]R. D. Levine and R. B. Bernstein, *Molecular Reaction Dynamics and Chemical Reactivity* (Oxford University Press, London, 1987).

[51]J.-C. Nieh and J. J. Valentini, Phys. Rev. Lett. **60**, 519 (1988).
[52]D. L. Phillips, H. B. Levene, and J. J. Valentini, J. Chem. Phys. **90**, 1600 (1989).
[53]D. G. Truhlar and C. J. Horowitz, J. Chem. Phys. **68**, 2466 (1978); **71**, 1514 (E) (1979).
[54]O. Siegbahn and B. Liu, J. Chem. Phys. **68**, 2457 (1978).
[55]From thermal conductivity measurements in *CRC Handbook of Chemistry and Physics* (CRC, Cleveland, 1975), 55th Ed., p. F206.